# Z-Budget:

## Sub-Domain Water Budgeting Post-Processor for IWFM

## Theoretical Documentation and User's Manual

**Hydrology Development Unit**
**Modeling Support Branch**
**Bay-Delta Office**
**February, 2010**

## Table of Contents

## List of Figures

## List of Tables

# 1. Introduction

State of California Department of Water Resources (DWR) has been developing and maintaining an integrated regional groundwater and surface water modeling tool in order to assist its water resources management and planning studies. The simulation of the groundwater elevations using the Galerkin finite element method (GFEM) lies at the core of this model. The model, named Integrated Water Flow Model (IWFM), is a generic simulation tool that can be applied to any groundwater basin (DWR 2007). The users of IWFM include DWR staff, consulting companies, other state and federal agencies, and universities. The applications of IWFM include California Central Valley Simulation Model (C2VSIM), Western San Joaquin Basin Model (WESTSIM), and applications to the Merced Basin and Butte County.

Over the past years IWFM users have requested the development of a feature that allows the detailed listing of inflow and outflow components at sub-domains of a modeled groundwater basin, a feature similar to the ZoneBudget post-processor (Harbaugh 1990) to the well known MODFLOW (McDonald and Harbaugh 1988). The need stemmed from the fact that modeling studies required the quantification of the changes in the subsurface flow rates between adjacent sub-domains (usually defined by political boundaries such as water districts, counties, states, etc.) of the modeled groundwater basin due to changing surface/subsurface water management practices in these sub-domains. The need to examine the detailed inflow/outflow components at a sub-domain level during calibration and verification stages of a modeling study was another reason behind the need for such a feature.

This report details a computer program, named Z-Budget, which is developed as a post-processing tool to be used with IWFM. Z-Budget recovers the subsurface flows at element interfaces given the groundwater heads computed by IWFM. Usage of Z-Budget will allow DWR, as well as other users of IWFM, to quantify the effects of water management practices utilized in one water district on the water resources of the adjacent districts, leading to a better analysis of the water management policies and practices.

## 2. Theoretical Background

Unlike in finite difference models such as MODFLOW, the recovery of groundwater fluxes based on the simulated groundwater heads in finite element models such as IWFM is not a straightforward task. Conventionally, the flux field is computed with Darcy's law by differentiating the head field that is calculated by the GFEM directly. The flux field generated by the conventional method is continuous over elements but discontinuous at the element interfaces violating the principle of mass conservation in both local and global sense. Yeh (1981) reported global mass balance errors of up to 30% when the conventional method is used. He suggested that the finite element procedure that is used to simulate the groundwater head field also be applied to Darcy's law with the fluxes as the state variables. Although his method produced better results, test problems still showed mass balance errors of 2-9% (Yeh 1981). Furthermore, Yeh's method increases the computer run times substantially since the number of equations to be solved is tripled for two-dimensional (quadrupled for three-dimensional) problems due to the inclusion of fluxes as state variables. Commenting on Yeh's work, Lynch (1984) showed that precise global mass balance can be achieved in GFEM by

proper treatment of the Dirichlet boundary conditions. He pointed out that the common practice of discarding Galerkin equations – the discrete version of the conservation equation – along Dirichlet boundaries violates the mass balance by requiring that these fluxes be approximated by utilizing the conventional method of differentiating the numerical head solution. He showed that retaining the Galerkin equation at Dirichlet boundaries as the equation for the flux resulted in precise global mass balance. Similar observations have been made by other researchers (Carey 1982, Carey et al. 1985, Hughes et al. 2000, Berger and Howington 2002, Carey 2002). In fact, the same idea can be used to compute the internal fluxes, i.e. once the groundwater head at an internal node is computed with GFEM, that node can be treated as a Dirichlet boundary and the Galerkin equation at the node can be solved for the flux (Hughes et al. 2000, Carey 2002). Cordes and Kinzelbach (1992) used a post-processing method where the elements were subdivided into patches and individual fluxes for each patch were computed by assuming that the flow field was irrotational. The mixed hybrid finite element method is another technique that was proposed to compute continuous flux fields (Chavent and Jaffré 1986). In this method, both head that is assumed piecewise constant over each element and flux that is associated with element edges are computed directly by solving the mass conservation equation and Darcy's law, simultaneously. In a study comparing the performance of the mixed hybrid finite element method and the post-processing technique of Cordes and Kinzelbach (1992), Mosé et al. (1994) claimed that the latter led to a substantial increase in CPU time.

Z-Budget utilizes an efficient post-processing technique that combines several approaches that are described in the studies mentioned above. Once the groundwater

heads are computed by IWFM at each finite element node, Z-Budget treats each node as a Dirichlet boundary node with a specified head and uses the irrotationality of the flow field to compute flows across element interfaces, i.e. normal flux integrated along each element interface. Once IWFM is run for a simulation period and the flow rates at every element interface is computed, the user can group one or more elements into individual zones and list the detailed inflow/outflow components into each of these zones. In the following sections, the mathematical development of the underlying theory for Z-Budget will be detailed.

In IWFM, the depth-integrated conservation equation for groundwater flow is expressed as (DWR 2007)

$$S\frac{\partial h}{\partial t} + \nabla \cdot \mathbf{q} = f \qquad (1)$$

where S is the storativity (specific yield for an unconfined aquifer and storage coefficient for a confined aquifer) (dimensionless), $h = h(x, y, t)$ is the groundwater head (L), $\mathbf{q} = q_x \mathbf{e_x} + q_y \mathbf{e_y}$ is the depth-integrated flux, or simply flux, in vector form with $\mathbf{e_x}$ and $\mathbf{e_y}$ being the unit vectors in the x and y directions respectively ($L^2/T$), f is the source/sink term (L/T), $\nabla = (\partial/\partial x)\mathbf{e_x} + (\partial/\partial y)\mathbf{e_y}$ is the del operator (1/L), and t is time (T). In (1), $f = f(h, x, y, t)$ is a general source/sink term that may be a combination of point sources (e.g. pumping and injection wells), distributed sources (e.g. recharge from an overlaying vadose zone) and head dependent sources (e.g. tile drains, stream-groundwater interaction).

Using the Darcy's law, $\vec{q}$ can be represented as

$$\mathbf{q} = -T\nabla h \qquad (2)$$

and

$$T = K\left[\min\left(h, z_u\right) - z_b\right] \tag{3}$$

where T is the aquifer transmissivity ($L^2/T$), $K = K\left(x, y\right)$ is the hydraulic conductivity (L/T), $z_u$ and $z_b$ are the top and bottom aquifer elevations (L), respectively. Equation (3) represents transmissivity for both confined and unconfined aquifers.

Integrating (1) in a weak sense for an arbitrary domain $\Omega$, using the Green's theorem and rearranging the resulting expression gives

$$\int_{\Gamma} -\mathbf{q}\cdot\mathbf{n}\omega d\Gamma = \int_{\Gamma} \theta\omega d\Gamma = \int_{\Omega}\left(S\frac{\partial h}{\partial t}\omega - \mathbf{q}\cdot\nabla\omega - f\omega\right)d\Omega \tag{4}$$

where $\omega = \omega\left(x, y\right)$ is an admissible test function, $\Gamma$ is the boundary surrounding the domain $\Omega$, $\mathbf{n}$ is the outward unit vector perpendicular to $\Gamma$ and $\theta = -\mathbf{q}\cdot\mathbf{n}$ is the flux normal to $\Gamma$. Based on the boundary conditions, $\Gamma$ can be divided into Dirichlet boundary, $\Gamma_D$, where groundwater head is specified and Neumann boundary, $\Gamma_N$, where normal flux, $\theta_N$, is specified. Expressing the boundary integral in (4) as the summation of integrals over the Dirichlet and Neumann boundaries and substituting Darcy's law into (4), the exact normal flux at the Dirichlet boundary, $\theta_D$, satisfies the following equality:

$$\int_{\Gamma_D} \theta_D\omega d\Gamma_D = \int_{\Omega}\left(S\frac{\partial h}{\partial t}\omega + T\nabla h\cdot\nabla\omega - f\omega\right)d\Omega - \int_{\Gamma_N}\theta_N\omega d\Gamma_N \tag{5}$$

(5) is the weak formulation of the groundwater flow conservation equation on which GFEM is based. It should be noted that even though the exact normal flux at the Dirichlet boundary appears in (5), no information can be deduced as to the functional

form of $\theta_D$. The left hand side of (5) actually represents the net flow through the Dirichlet boundary in a weak sense.

In GFEM, a set of finite element basis functions $\{\omega_i\}$ on a discretization of $\Omega$ is introduced, and the head and test functions are approximated as (Allen et al. 1988)

$$\tilde{h} = \sum_{i=1}^{m} h_i(t)\omega_i(x,y) \tag{6}$$

$$\tilde{\omega} = \omega_i(x,y), \quad i = 1,\cdots,m \tag{7}$$

where m is the number of nodal points based on the discretization. In the remainder of the mathematical development it will be assumed that the basis functions used in (7) are linear Lagrange basis functions since they are a typical choice in most GFEM applications. Substitution of (6) and (7) into (5) generates a set of ordinary differential equations:

$$\begin{aligned} Q_i = \int_{\Gamma_D} \theta_D \omega_i d\Gamma_D = \int_{\Omega} \left( S\omega_i \sum_{j=1}^{m} \frac{\partial h_j}{\partial t}\omega_j + T\sum_{j=1}^{m} h_j \nabla\omega_j \cdot \nabla\omega_i - f\omega_i \right) d\Omega \\ - \int_{\Gamma_N} \theta_N \omega_i d\Gamma_N \quad , \quad i = 1,\cdots,m \end{aligned} \tag{8}$$

where $Q_i$ can be interpreted as the flow through a section of the Dirichlet boundary, $\Gamma_D$, associated with boundary node i. Only one type of boundary condition, either Dirichlet or Neumann, can be specified at a node. If a Dirichlet boundary condition is specified at node i, then the term that represents the flux integral over the Neumann boundary, $\Gamma_N$, vanishes in (8). On the other hand, if a Neumann boundary condition is specified, then $Q_i$

becomes zero. For internal nodes, test functions vanish on the boundary, rendering the boundary integrals in (8) as zero.

Further modifications on (8) are performed before attempting to solve the system of equations: a mass lumping technique may be applied on the time derivative (Allen et al. 1988); the time derivative may be discretized using finite difference method; transmissivity may be approximated as a piecewise constant over elements, as an expression similar to the one given in (6) or simply as a constant over the entire domain. Finally, equation (8) is converted into a set of algebraic equations that are relatively easy to solve. Regardless of the specific modifications, (8) is the expression for groundwater flow at the Dirichlet boundary that is consistent with the GFEM. It is, in fact, the Galerkin equation at the Dirichlet boundary that needs to be retained as the flow equation in order to achieve a precise mass balance (Lynch 1984). If there are $m_D$ boundary nodes specified as Dirichlet nodes, then equation (8) represents $m_D$ equations to be solved simultaneously to recover the flow at the Dirichlet boundary. During the application of GFEM, the right hand side of (8) is evaluated to compute the groundwater heads. Therefore, calculation of the flow at the Dirichlet boundary nodes requires a small amount of computation time and the mass balance obtained by using these flows is accurate up to the machine precision (Hughes et al. 2000).

Equation (8) is written for an arbitrary domain, $\Omega$, and its enclosing boundary, $\Gamma$. Therefore, it is valid for any collection of elements: the set of all elements that approximate the entire model domain, a subset of these elements or even an individual element. Figure 1.a depicts an example discretization of global domain, $\Omega_g$, and two groups of elements that represent sub-domains, $\Omega_1$ and $\Omega_2$, and their respective enclosing

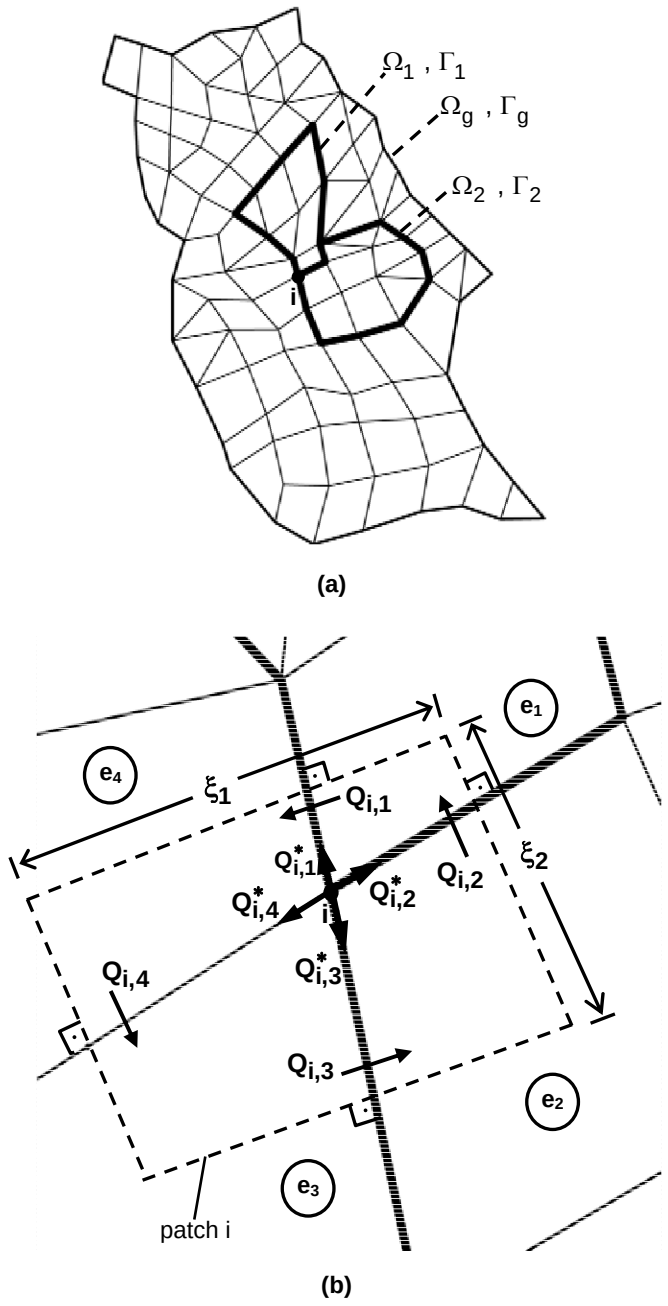


**Figure 1** Descriptive schematics of (a) discretizations of global and two subdomains, (b) enlarged view of vicinity of node i

boundaries $\Gamma_g$, $\Gamma_1$ and $\Gamma_2$. When (8) is written for any of the sub-domains, the head values at the sub-domain boundary nodes that are obtained from the application of GFEM can be treated as Dirichlet boundary nodes. Then, (8) produces the flows at boundary

nodes of the sub-domain. As such, (8) is a post-processing technique for the recovery of the boundary flows based on the nodal head values and it is consistent with the GFEM approximation.

The aim is to utilize equation (8) to compute flows through each of the element faces of the finite element grid so that a precise mass balance for arbitrarily defined collections of elements as well as the flows between adjacent element collections can be computed. To achieve this, however, (8) alone can not be used and it is necessary to utilize further information such as the irrotationality of the flow field. To demonstrate this point, node i in Figure 1.a, which lies between two sub-domains, will be considered. Figure 1.b shows an enlarged view of the vicinity of node i and the corresponding patch with $e_1$ and $e_2$ as the elements that belong to sub-domains 1 and 2, respectively. Patch i in Figure 1.b is constructed by connecting the lines that perpendicularly cross element faces at mid-points. When (8) is written for element $e_1$ at node i, it represents the conservation of mass at the intersection of patch i and element $e_1$:

$$Q_i^{e_1} = \int_{\Omega^{e_1}} F_i d\Omega^{e_1} = Q_{i,2} - Q_{i,1} \qquad (9)$$

where $Q_i^{e_1}$ is the flow that crosses the patch boundary (dashed line in Figure 1.b) in element $e_1$, $F_i$ is the integrand in (8), $\Omega^{e_1}$ is the domain of element $e_1$, $Q_{i,1}$ is the flow through half of the interface between elements $e_1$ and $e_4$, and $Q_{i,2}$ is the flow through half of the interface between elements $e_1$ and $e_2$, as depicted in Figure 1.b. Since the exact normal flux expressed as a function of distance along the faces of element $e_1$ is not known, $Q_{i,1}$ and $Q_{i,2}$ can not be determined directly; (9) represents a single equation with two unknowns. Writing (8) also for element $e_2$ at node i, produces two equations with

three unknowns, namely $Q_{i,1}$, $Q_{i,2}$ and $Q_{i,3}$. Finally, expressing (8) for all the surrounding elements of node i generates four equations with four unknowns but the resulting system of equations is underdetermined, i.e. one of the equations in the system is a linear combination of the rest:

$$\begin{bmatrix} -1 & 1 & 0 & 0 \\ 0 & -1 & 1 & 0 \\ 0 & 0 & -1 & 1 \\ 1 & 0 & 0 & -1 \end{bmatrix} \begin{Bmatrix} Q_{i,1} \\ Q_{i,2} \\ Q_{i,3} \\ Q_{i,4} \end{Bmatrix} = \begin{Bmatrix} Q_i^{e1} \\ Q_i^{e2} \\ Q_i^{e3} \\ Q_i^{e4} \end{Bmatrix} \tag{10}$$

To close the system of equations in (10), irrotationality of the flow field will be assumed. Similar approaches have also been taken by Cordes and Kinzelbach (1992), and Chou et al. (2004). The irrotationality of the flow field can be expressed as

$$\nabla \times \mathbf{q} = \frac{\partial q_y}{\partial x} - \frac{\partial q_x}{\partial y} = \nabla \cdot \mathbf{q}^* = 0 \tag{11}$$

where $\mathbf{q}^* = q_y \mathbf{e_x} - q_x \mathbf{e_y}$. Writing equation (11) in a weak sense using the finite element basis functions and applying the Green's theorem gives

$$Q_i^* = \int_\Gamma \mathbf{q}^* \cdot \mathbf{n} \omega_i d\Gamma = \int_\Omega T \sum_{j=1}^{m} \left( h_j \nabla^* \omega_i \cdot \nabla \omega_j \right) d\Omega \;\; ; \;\; i = 1, \cdots, m \tag{12}$$

where $Q_i^*$ is the circulation at node i (Bear 1988) and $\nabla^* = (\partial/\partial y)\mathbf{e_x} - (\partial/\partial x)\mathbf{e_y}$. Since $\mathbf{q}^* \cdot \mathbf{n} = \mathbf{q} \cdot \mathbf{n_T}$, where $\mathbf{n_T}$ is the unit tangent at the boundary in a counter clockwise direction, (12) represents the line integral of the tangential flux at the boundary, $\Gamma$. The evaluation of (12) requires the additional computation of the integral

$$\int_\Omega \nabla^* \omega_i \cdot \nabla \omega_j \, d\Omega \quad ; \quad i, j = 1, \cdots, m \tag{13}$$

where it is assumed that the transmissity is approximated so that it can be taken out of the integral. Regardless of the approximation of the transmissivity, the integral in (13), or any variants of it due to a particular approximation, needs to be computed only once at the beginning of the simulation, and should not increase the computer run times significantly.

Adopting the convention where the counter clockwise direction is positive and writing (12) for element $e_1$ at node i (Figure 1.b) gives

$$Q_i^{*,e_1} = \int_{\Omega^{e_1}} G_i d\Omega^{e_1} = Q_{i,2}^* - Q_{i,1}^* \qquad (14)$$

In (14), $Q_i^{*,e_1}$ is the integral of the tangential flux along the part of the patch boundary that lies in element $e_1$ (Figure 1.b), $G_i$ is the integrand in (12), $Q_{i,2}^*$ is the integral of the tangential flux along half of the interface between elements $e_1$ and $e_2$, and $Q_{i,1}^*$ is the integral of the tangential flux along half of the interface between elements $e_1$ and $e_4$. Since the circulation about any closed curve at any location in an irrotational flow has to be zero (Bear 1988), $Q_i^{*,e_1}$ counter-balances the integral of the tangential flux along the faces of element $e_1$ that fall in patch i, i.e. $Q_{i,2}^* - Q_{i,1}^*$. When (12) is written at internal nodes, the test functions vanish at the global boundary and $Q_i^*$ in (12) becomes zero. This result is consistent with the theory that the circulation about a closed curve in an irrotational flow field is zero. On the other hand, a closed curve around a boundary node can not be specified, and expressing (12) at a boundary node produces a non-zero value.

To utilize (12) as a closure to the system of equations listed in (10), it is necessary to express the components of the circulation, $Q^*_{i,k}$, in the patch in terms of the flow terms, $Q_{i,k}$. For this purpose, it will be assumed that the normal flux at the element face that falls in the patch is constant and $Q_{i,k}$ can be expressed in terms of this normal flux. For instance, $Q_{i,1}$ in Figure 1.b can be used to express the constant normal flux at the half of the interface between elements $e_1$ and $e_4$:

$$Q_{i,1} = \int_{\Gamma_{e_1,e_4}} \theta\omega_i d\Gamma \cong \theta^i_{e_1,e_4} \int_{\Gamma_{e_1,e_4}} \omega_i d\Gamma = \theta^i_{e_1,e_4} \frac{L_{e_1,e_4}}{2} \tag{15}$$

or

$$\theta^i_{e_1,e_4} = \frac{2}{L_{e_1,e_4}} Q_{i,1} \tag{16}$$

where $\theta^i_{e_1,e_4}$ is the constant patch flux normal to the element face that falls into patch i, $\Gamma_{e_1,e_4}$ is the interface between the two elements and $L_{e_1,e_4}$ is the length of the interface. As noted earlier, (16) is obtained assuming that the linear Lagrange basis is used for $\omega_i$. A similar expression can be written for the normal flux at the interface between elements $e_1$ and $e_2$ that falls into patch i (Figure 1.b):

$$\theta^i_{e_1,e_2} = \frac{2}{L_{e_1,e_2}} Q_{i,2} \tag{17}$$

Next, it will be assumed that the patch flux normal to the element face is equal to the flux that is tangent to the patch boundary and it is spatially constant along the corresponding side of the patch. For example, in Figure 1.b $\theta^i_{e_1,e_4}$ is assumed to be the flux tangent to the side of the patch with length $\xi_1$. Similarly, $\theta^i_{e_1,e_2}$ is assumed to be the

flux tangent to the side of the patch with length $\xi_2$ (Figure 1.b). Finally, using the expressions for the tangent fluxes the irrotationality at an internal node can be written as

$$\sum_{k=1}^{c_i} \frac{2\xi_k}{L_{i,k}} Q_{i,k} = 0 \qquad (18)$$

where $c_i$ is the number of element faces that connect at node i, $L_{i,k}$ is the length of the element face k, and $\xi_k$ is the length of the patch boundary that crosses element face k perpendicularly. (18) corresponds to (12) where the tangent fluxes are approximated in terms of normal fluxes, as described above.

For a boundary node a closed curve can not be specified and application of (12) and (18) generates a non-zero value:

$$\sum_{k=1}^{c_i} \frac{2\xi_k}{L_{i,k}} Q_{i,k} = \int_{\Omega} T \sum_{j=1}^{m} \left( h_j \vec{\nabla}^* \omega_i \cdot \vec{\nabla} \omega_j \right) d\Omega \qquad (19)$$

The right-hand side of (19) can easily be computed by using the head and transmissivity values obtained from the solution of (1) using GFEM.

Replacing the last equation of the system described in (10) by (18) or (19) for internal and boundary nodes, respectively, produces a well-posed set of equations that can be solved very efficiently. The system of equations is defined for each node and can be solved locally independent from the equation systems defined for other nodes. For an element face identified with nodes i and j, two flow terms will be computed: one for node i that crosses through half of the element face located in patch i, and the other for node j that crosses the other half of the face located in patch j. Once the two flow terms are computed they can be summed to obtain the net flow through the entire element face defined by nodes i and j.

The preceding mathematical development assumes that the flow field is irrotational. It can be shown that the depth-integrated conservation equation (1) always satisfies the irrotationality condition (Bear 1988). Therefore, utilizing the above approach can be used under any circumstances as long as (1) is used to model the groundwater flow. However, the approach detailed above is general enough so that it is applicable to any form of the groundwater flow equation as long as the flow field is irrotational.

## 3. Verification of Methodology

The accuracy and the convergence characteristics of Z-Budget are now demonstrated by comparing the results to the analytic solutions of several test problems.

*Example 1*

The first example deals with the radial flow to a well that fully penetrates a confined aquifer with a uniform thickness of 100 m. The aquifer is homogeneous, isotropic and has an infinite extent. The hydraulic conductivity and the specific storage of the aquifer are $2.3 \times 10^{-5}$ m/sec and $7.5 \times 10^{-6}$ $m^{-1}$, respectively. The well diameter is small and the storage in the wellbore can be neglected. The pumping rate is constant at 0.004 $m^3$/sec. The analytical expressions for the drawdown and the flow at a distance from the well can be obtained by using the Theis method (Theis 1935).

By symmetry, the drawdown and the flow were simulated only in a single quadrant of the domain using non-uniform grid spacing. In the angular direction the quadrant was discretized into four equal regions. The grid spacing in the radial direction

was increased at specified intervals as the distance from the well increased. For the purposes of numerical simulation the infinite extent of the aquifer was approximated by setting specified head boundary conditions at 20000 m away from the well. The initial groundwater head and the specified head at the boundary were each set to 150 m. The simulation period was 1 day with 10 second time steps. To assess the performance of Z-Budget the flow rate simulated at a radius of 55 m from the well is compared to the flow rate computed using the Theis (1935) solution. To further check the rate of convergence of the results from Z-Budget to the analytical solution, the same problem was solved with a successively refined grid in the radial direction. The discretization in the angular direction was kept the same for all grid resolutions.

Figure 2.a shows a comparison of the flow rate at a radius of 55 m from the well computed with the Theis method and Z-Budget at the coarsest grid resolution tested. It is obvious that Z-Budget gives excellent results even at a coarse grid resolution. For the purpose of establishing the convergence rate of Z-Budget to the analytical solution, Figure 2.b depicts the logarithmic plots of the grid size versus error in the flow as well as the drawdown. The error term both for flow and drawdown is computed as the normalized $L^2$-norm of the error vector for the simulation period:

$$E = \frac{\sqrt{\sum_{i=1}^{tmax} \left( f_{s_i} - f_{a_i} \right)^2}}{\sqrt{\sum_{i=1}^{tmax} \left( f_{a_i} \right)^2}} \qquad (20)$$

where E is the normalized $L^2$-norm of the error vector, tmax is the maximum number of time steps for the simulation period, $f_{s_i}$ is the value (flow or drawdown) at the *i*th time

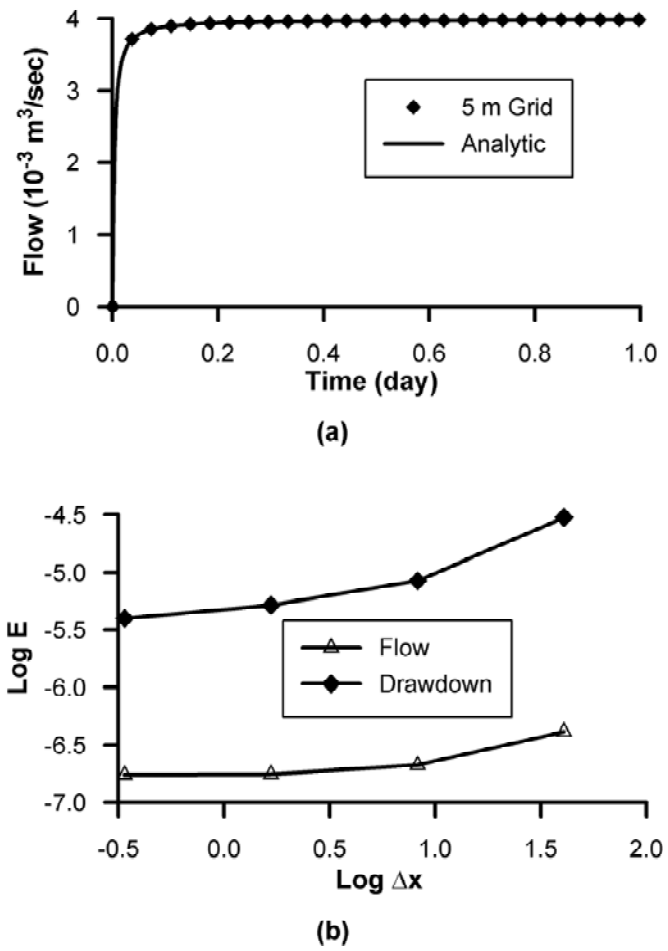


**Figure 2** Results for example 1: (a) Flow comparison at 55 m from the well and (b) log-log plot of grid size versus error in flow and drawdown

step computed by the numerical simulation, and $f_{a_i}$ is the corresponding value at the *i*th time step computed by the Theis method.

It should be noted that for all tested grid sizes the error in flow is very small (Figure 2.b). Figure 2.b shows that the convergence rate for the flow is non-linear and logarithm of the flow error converges to a constant at around –6.75. This is expected because the infinite-aquifer assumption used for the analytical solution is approximated with a finite aquifer extent in the numerical solution. Therefore, a discrepancy between

the analytical and the numerical solutions will always be observed, and it is logical that the difference between the two solutions converges to a non-zero constant as the grid is refined. The log-log plot of the drawdown versus error shows a similar trend in the convergence rate. Comparison of the drawdown versus error and flow versus error plots also reveals that the convergence rate for the flow is about half the convergence rate for the drawdown. Overall, Z-Budget to recover the flow rates at element faces in a Theis aquifer performs very well.

*Example 2*

The second example was designed to test the performance of Z-Budget in heterogeneous aquifer conditions. It has been reported that as the level of heterogeneity increases the accuracy of the conventional method to recover flow rates also decreases. The setup for this example is shown in Figure 3.a. An unconfined aquifer lies between two lakes. The length of the aquifer in the x-direction, $L_x$, is 10 km and in the y-direction, $L_y$, is 2 km. The surface elevations of the lakes are constant but different from each other. The lake on the right side of the aquifer has an elevation of $H_1$ = 200 m and the left-hand-side lake has an elevation of $H_2$ = 50 m. There is no flow across the other two sides of the aquifer. The specific yield, S, of the aquifer is 0.25. The aquifer is composed of vertical strips of soil that are 200 m wide with different hydraulic conductivities. The plan view of the aquifer and the finite element grid used in the simulation is shown in Figure 3.b. The grid sizes in x and y directions, $\Delta x$ and $\Delta y$ respectively, are both 200 m. To simulate heterogeneous aquifer conditions, each vertical strip of soil was assigned a random hydraulic conductivity, K. The randomly

heterogeneous hydraulic conductivity field was assumed log-normally distributed, uncorrelated, and characterized by its coefficient of variation, $\rho_K$, defined as

$$\rho_K = \frac{\sigma_K}{\overline{K}} \tag{21}$$

where $\sigma_K$ and $\overline{K}$ are the standard deviation and the mean of the random hydraulic conductivity field, respectively. The performance of Z-Budget to compute the element face flows was tested for several degrees of heterogeneity with $\rho_K$ taken as 0.0 (homogeneous case), 0.5, 1.0, 2.0 and 3.0. For all test cases $\overline{K}$ was taken to be 100 m/day.

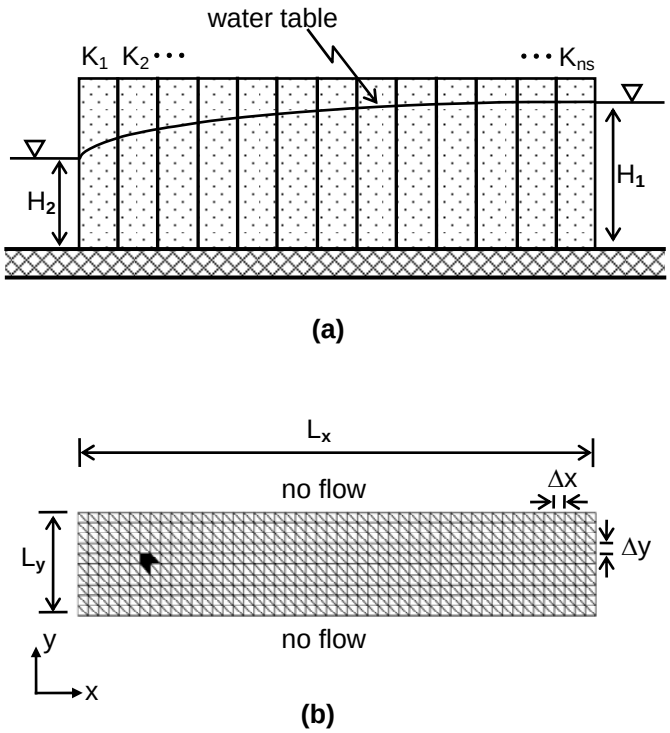


**Figure 3** Definition sketch for example 2: (a) cross section of a heterogeneous aquifer between two lakes and (b) simulation grid (shaded area represents the test sub-domain)

Since there is no variation in the hydraulic conductivity in the y-direction and the upper and lower boundary conditions are symmetric (Figure 3.b), the flow between the two lakes is essentially one dimensional. The analytical expression for the flux at the steady state of this problem can be expressed as

$$q = \frac{\left(H_2^2 - H_1^2\right)}{\left(2W_x \sum_{i=1}^{ns} \frac{1}{K_i}\right)} \qquad (22)$$

where $W_x$ = 200 m is the width of soil strips in x-direction, ns = 50 is the total number of soil strips and $K_i$ is the random hydraulic conductivity assigned to the $i^{th}$ strip. $H_1$ and $H_2$ are the specified head boundary conditions as defined earlier (Figure 3.a).

To assess its performance, the results of Z-Budget are compared with the analytical solution as well as the conventional method of computing the flows at element faces. It should be noted that, since the flow computed by the conventional method is discontinuous at an internal element interface, the average of the flows on each side of the interface is used in the comparisons.

First, the behavior of the simulated flows at the boundary element faces is analyzed. Figure 4 shows a comparison of the flow computed at each of the boundary element faces, starting at the lower left boundary face, by using the analytical, proposed and conventional methods for $\rho_K$ = 1.0. It is obvious that the conventional method of computing flows violates the no flow conditions at the upper and lower boundaries (see Figure 3 for boundary conditions). On the other hand, Z-Budget preserves the no flow boundary conditions except at the lower right and the upper left corners of the domain. This behavior is due to the grid used in the example. Even though the actual flow is one

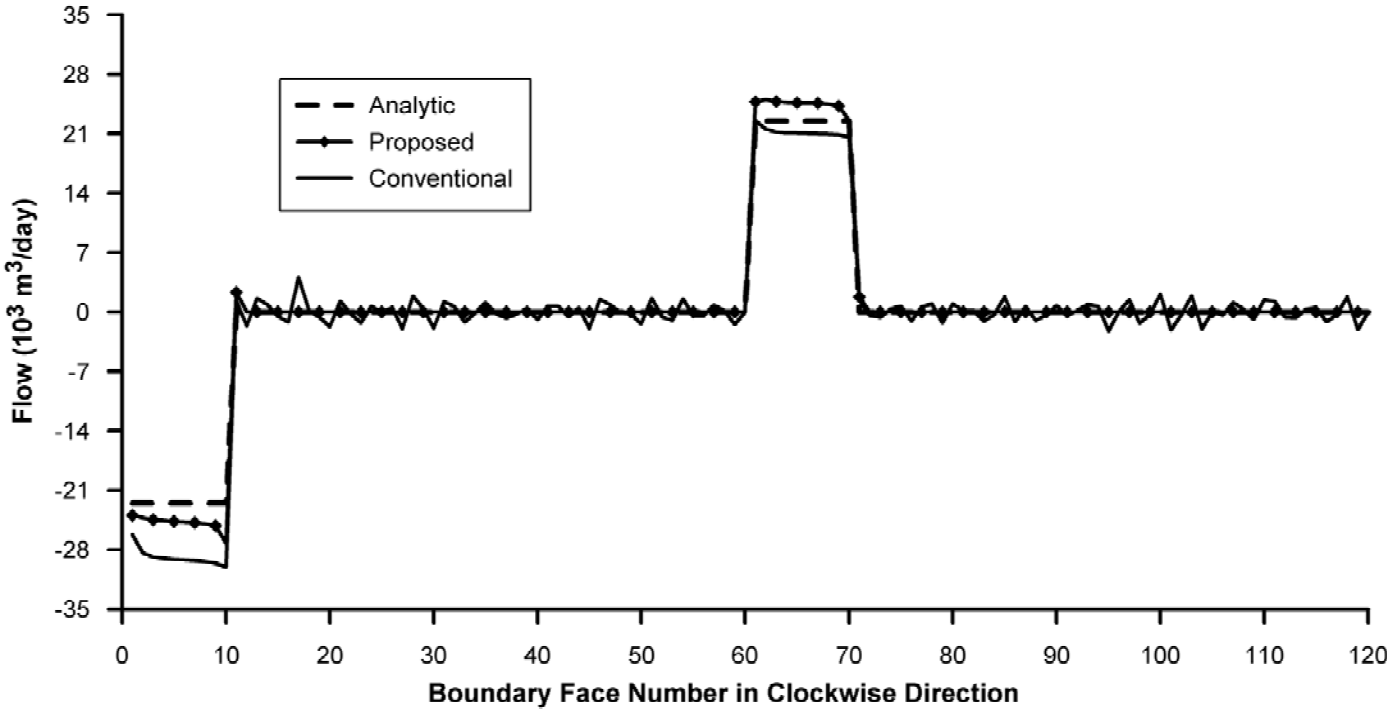


**Figure 4** Comparison of flows computed at the boundary element faces for $\rho_K = 1.0$

dimensional, the application of GFEM produces a small, artificial flow along the diagonal element faces specified in the finite element grid (Figure 3.b). Z-Budget correctly computes zero flows across the upper and lower boundary element faces except at the upper left and lower right corners of the domain where two different boundary conditions interface. This phenomenon is not observed at the lower left and upper right corners of the grid because the element faces are in alignment with the actual flow direction. At these corners, flow can only occur in either x or y direction along the horizontal or vertical faces, respectively. Z-Budget computes correct element face flows since no artificial diagonal flow is introduced at these locations.

Figure 5 shows the comparison of the normalized $L^2$ norm, computed using (20), of the error vectors for the boundary face flows computed by the proposed and conventional methods for differing levels of heterogeneity. As the level of heterogeneity increases the error in the boundary face flows produced by both of the methods also

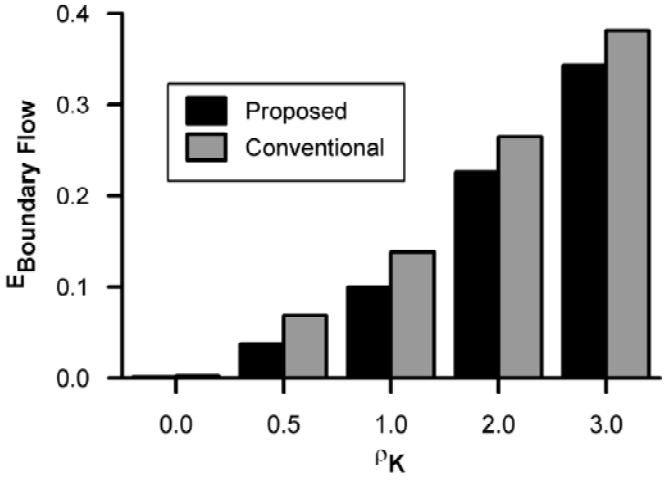


**Figure 5** Comparison of the error for boundary flows computed by the proposed and conventional methods for different levels of heterogeneity

increases. However, it can be seen that Z-Budget consistently produces more accurate flow results than the conventional method.

To assess the convergence rate of Z-Budget the initial grid was refined progressively by halving the grid spacing both in x and y directions for $\rho_K = 1.0$. Figure 6 shows the logarithm of the grid size versus the logarithm of the normalized $L^2$ norm, E (computed by using (20)), of the flow error computed at each element face by using the proposed and the conventional methods. It can be seen that Z-Budget has a slightly

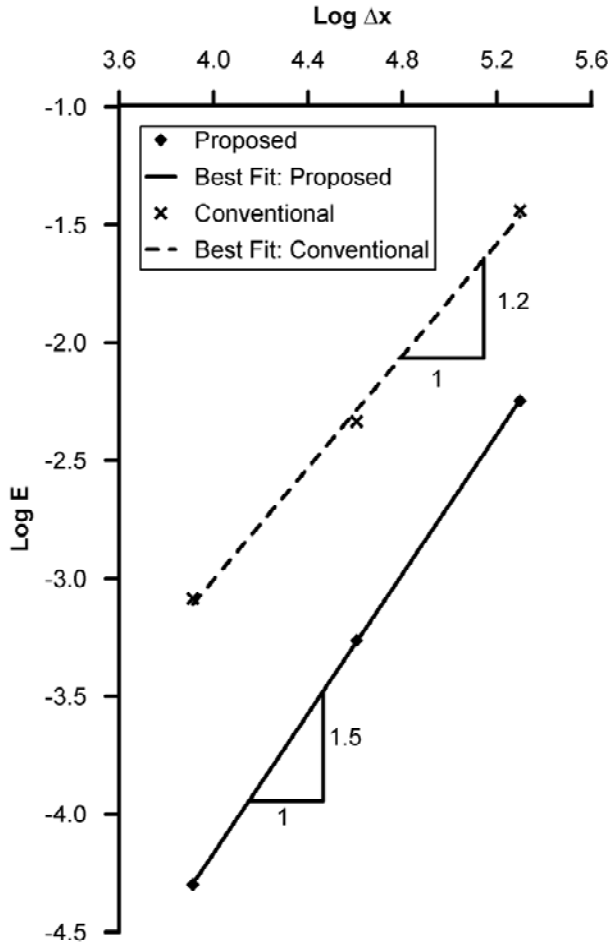


**Figure 6** Log-log plot of the grid size versus error in flow computed by the proposed and conventional methods for $\rho_K = 1.0$

higher convergence rate than the conventional method and its overall accuracy is better. The conventional method requires about 4 times more grid points than Z-Budget to achieve a comparable level of accuracy.

Yeh (1981) reported large discrepancies in the global mass balance when the flow rates computed by the conventional method were used. To further demonstrate the benefits of Z-Budget of flow recovery, Table 1 compares the total inflow and outflow to the aquifer computed by the analytic, conventional and proposed methods as well as the global mass balance error in the conventional method at different levels of heterogeneity with the grid size of 200 m. The conventional method produces increasing global mass balance errors of up to 45% as the heterogeneity increases whereas proposed method shows precise mass balance. It appears that as the heterogeneity increases the difference between the flow rates computed with analytic and proposed methods also increases. This suggests the necessity of using finer mesh as the heterogeneity of the aquifer increases. In the light of the discussion given in the preceding paragraph, Z-Budget would require 4 times fewer nodal points than the conventional method to achieve a certain level of accuracy with precise global mass balance.

One of the goals of this report is to demonstrate the ability of Z-Budget to recover element face flows based on the groundwater heads computed by GFEM so that mass balances can be established at the sub-domain level. Table 2 shows the performance of Z-Budget in computing the inflow and outflow rates into an arbitrarily chosen sub-domain for $\rho_K = 1.0$ at differing grid resolutions. The sub-domain is shown as the shaded area in Figure 3.b. Once again, Z-Budget achieves precise mass balance at sub-domain level whereas the conventional method generates up to 23% of mass balance error. Table

| $\rho_K$ | Total Inflow ($m^3$/day) | | | Total Outflow ($m^3$/day) | | | Mass Balance Error in Conventional (%) |
|---|---|---|---|---|---|---|---|
| | Analytic | Proposed | Conventional | Analytic | Proposed | Conventional | |
| 0.0 | 375,000 | 375,030 | 375,932 | 375,000 | 375,030 | 367,229 | 2.32 |
| 0.5 | 323,865 | 336,268 | 347,639 | 323,865 | 336,268 | 407,424 | -17.20 |
| 1.0 | 225,147 | 248,713 | 258,724 | 225,147 | 248,713 | 333,613 | -28.95 |
| 2.0 | 100,472 | 124,291 | 128,565 | 100,472 | 124,291 | 180,058 | -40.05 |
| 3.0 | 51,594 | 70,037 | 72,023 | 51,594 | 70,037 | 104,566 | -45.18 |

**Table 1** Total inflow and outflow rates computed by analytic, proposed and conventional methods, and the global mass balance error in the conventional method

2 also shows the convergence rate of Z-Budget at around 1.2. At the sub-domain level, the conventional method does not display a uniform convergence. It should be noted that, since the total inflow and outflow rates to and from the zone computed by the conventional method are not the same, their averages are used in computing the percent difference between the analytic and the conventional method in Table 2.As mentioned earlier, using Z-Budget to recover the flow rates by post-processing the groundwater heads computed by the GFEM increases the computer run-times minimally. In all test problems, the average increase in the computer run-times when Z-Budget was utilized was 1.25% with a maximum increase of 2.75% (Table 3). All the test problems were run on a 2.2 GHz Intel Pentium 4 processor with 1GByte RAM running with the Windows 2000 operating system. Even though it is difficult to measure the exact increase in the run-time due to the unpredictable effect of programs running in the background, it can be concluded that the extra computational time required by Z-Budget is insignificant. As mentioned earlier, this is due to the fact that most of the required information to compute the element face flows is already available through the application of the GFEM to

| Method | Δx (m) | Inflow ($m^3$/day) | Outflow ($m^3$/day) | Mass Balance Error (%) | Difference from Analytic (%) |
|---|---|---|---|---|---|
| Proposed | 50 | 45,903 | 45,903 | 0.00 | 1.94 |
| | 100 | 47,171 | 47,171 | 0.00 | 4.76 |
| | 200 | 49,362 | 49,362 | 0.00 | 9.62 |
| Conventional | 50 | 41,949 | 46,193 | -10.12 | -2.13 |
| | 100 | 41,957 | 48,039 | -14.50 | -0.07 |
| | 200 | 43,414 | 53,516 | -23.27 | 7.63 |

**Table 2** Inflow and outflow terms for the test sub-domain computed by the proposed and conventional methods

| $\rho_K$ | Computer Run-Times (sec) | | Increase in Run-time (%) |
|---|---|---|---|
| | Without Proposed Method | With Proposed Method | |
| 0.0 | 4.11 | 4.14 | 0.73 |
| 0.5 | 4.73 | 4.86 | 2.75 |
| 1.0 ($\Delta x$ = 200 m) | 6.05 | 6.09 | 0.66 |
| 1.0 ($\Delta x$ = 100 m) | 92.8 | 93.33 | 0.57 |
| 1.0 ($\Delta x$ = 50 m) | 1579.69 | 1609.55 | 1.89 |
| 2.0 | 8.5 | 8.56 | 0.71 |
| 3.0 | 10.91 | 11.06 | 1.37 |

**Table 3.** Computer run-times with and without the proposed method of flow recovery

compute the groundwater heads. Furthermore, Z-Budget requires the solution of a small system of equations, which can be performed very efficiently, at each node to recover the flow terms in a local sense.

## 4. Program Description

Z-Budget is written in FORTRAN 95 and includes several subroutines (Figure 7). A subroutine named Nflow.for is imbedded in the IWFM Simulation program. Nflow.for computes individual inflow/outflow components at each finite element due to model specific sources and sinks. This subroutine is also responsible of computing the element face flows based on the methodology described above. The inflow/outflow components for each element are saved in a binary file which is later used by the core Z-Budget program. The core program is responsible of aggregating inflow and outflow components for zones specified by the user by grouping one or more elements, and listing the aggregated results for each zone. In this section each of the Z-Budget subroutines will be described.

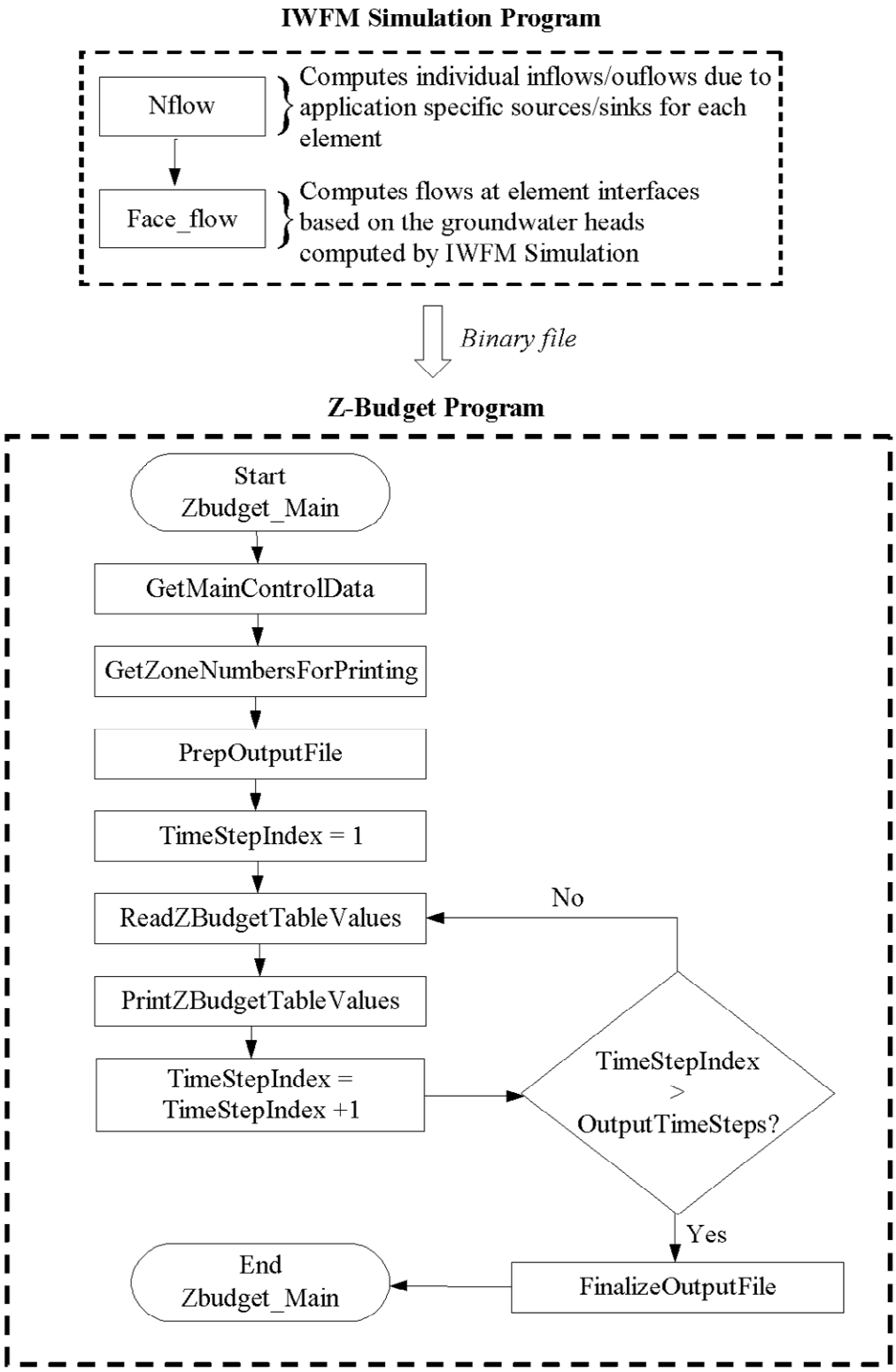


**Figure 7** Z-Budget flowchart

**Nflow** This subroutine is imbedded in the IWFM Simulation program. At the end of each time step, it computes individual inflow/outflow terms from application specific sources/sinks for each finite element. The sources and sinks are essentially the vertical inflows and outflows at each of the finite element at each aquifer layer. The computed values are stored in a binary file.

**Face_flow** This subroutine is also imbedded in IWFM simulation program. At the end of each simulation time step, the flow rates at each element face are computed based on the groundwater head values simulated by IWFM. The results are stored in the binary file.

**Zbudget_Main** This is the main program of the Z-Budget post-processor. It calls other subroutines for reading zone information, flow terms that are stored in the binary file by Nflow and Face_flow in IWFM Simulation program, and processing of the flow terms based on the zone information.

| | |
|---|---|
| **GetMainControlData** | This subroutine reads information from the main Z-Budget input file, the dimensions of the aquifer system that are saved in the Z-Budget binary file and calls other subroutines that construct the zonal definitions. |
| **GetZoneNumbersForPrinting** | This subroutine extracts the zone numbers from the main control file for which flux terms will be printed. |
| **PrepOutputFile** | This subroutine prepares the ASCII or DSS file for printing out the zonal flux terms and opens the temporary files used to store intermediate data during the processing of zonal flows. |
| **ReadZBudgetTableValues** | This subroutine reads flow terms stored in the binary file for a given simulation time step and aggregates them for each zone. |
| **PrintZBudgetTableValues** | This subroutine prints out the flow terms that are aggregated for each zone to intermediate storage files. |
| **FinalizeOutputFile** | This subroutine reads processed zonal flows from each of the intermediate files and combines them in the final ASCII or DSS file, whichever is specified for output. |

## 4.1. Input Files

The main control input file and the binary file that is generated during the execution of the IWFM Simulation program are required to run the Z-Budget post-processor.

The main input file contains the information about the name of the binary file from which flow terms will be read in, the extent of the zone numbering which will be explained later in this section, the conversion factor and unit names for the printed results, the starting and ending time steps for which the detailed water budget for each zone will be listed, the name of the DSS output file and the element and, if applicable, aquifer layer numbers that make up each zone.

The following is a list of variables that appear in the main input file for Z-Budget.

| | |
|---|---|
| BINFILE | The name of the binary file which is created by the IWFM Simulation program and stores the inflow and outflow terms for each element at each aquifer layer. |
| DSSFILE | The name of the DSS file which will be used to print out the zonal flow terms. If left blank, the zonal flows will be printed to an ASCII file. |
| ZEXTENT | Flag to identify the extent of the zone numbering. Enter 1 if zone numbering is defined in horizontal plane and applies to all aquifer layers in the vertical, enter 0 if different zone numbers will be specified for each aquifer layer. When ZEXTENT is set to 1, the zone number that is specified for each element is applied to all aquifer layers. In this case zones extend from the ground surface |

| | |
|---|---|
| | to the bedrock. When ZEXTENT is set to 0, then the user has to specify the element number and the aquifer layer in which the element lies when assigning zone numbers. This option allows the user to specify three-dimensional zones. |
| FACTVLOU | Factor to convert the volumetric unit of values stored in the binary input file to the desired unit of output. The unit of the values stored in the binary file is the same as the unit that is used in IWFM Simulation program internally. |
| UNITVLOU | Unit of the printed results. |
| CACHE | Cache size in terms of number of values stored in the memory for time series data output before the results are flushed into the output file. This variable has a significant impact on the speed of Z-Budget post-processor if a DSS file is being used for output. |
| TBEGIN | If the Simulation part of IWFM was run using the non-time tracking option, then this variable is used to specify the starting time step for which zonal flow terms will be printed. If Simulation part of IWFM was run using the time tracking option, then this variable should be commented out. |
| TLAST | If the Simulation part of IWFM was run using the non-time tracking option, then this variable is used to specify the ending time step for which zonal flow terms will be printed. If Simulation part of IWFM was run using the time tracking option, then this variable should be commented out. |

| | |
|---|---|
| BDT | If the Simulation part of IWFM was run using the time tracking option, then this variable is used to specify the starting date and time for which zonal flow terms will be printed. If Simulation part of IWFM was run using the non-time tracking option, then this variable should be commented out. |
| EDT | If the Simulation part of IWFM was run using the time tracking option, then this variable is used to specify the ending date and time for which zonal flow terms will be printed. If Simulation part of IWFM was run using the non-time tracking option, then this variable should be commented out. |
| IE | Element number for which a zone number is assigned. Only the elements that are contained in zones need to be listed. For instance, if a single zone in the model domain needs to ne identified, only the elements that fall in this zone need to be listed. The element numbers can be listed in any order. If ZEXTENT is set to 1 (i.e. zone numbering is defined for horizontal plane and will be used for all aquifer layers), an element number can not be listed more than once, otherwise an error will occur. If ZEXTENT is set to 0 (i.e. different zone numbering is specified for each aquifer layer), then same element number can be listed more than once but the layer numbers (specified in the variable LAYER that will be explained later in this section) corresponding to this element should be different. |

| | |
|---|---|
| LAYER | Aquifer layer number at which element IE is located. If ZEXTENT is set to 1, skip this variable. Otherwise incorrect zone numbers will be assigned to elements. If ZEXTENT is set to 0, then LAYER has to be specified. |
| ZONE | Zone number which element IE (at layer LAYER if ZEXTENT is set to 0) belongs to. By default all elements at all aquifer layers are assigned the zone number –99. Elements can be assigned any integer zone numbers except –99. The zone numbers do not have to be sequential. |
| ZPRINT | Zone numbers for which detailed water budget will be printed. The zone numbers listed under this variable must be one of the numbers that are listed under variable ZONE or –99. If a zone number that was not specified under ZONE is listed, a warning message will be generated and print-out for this zone will be suppressed. |

```
C*******************************************************************************
C
C                  INTEGRATED WATER FLOW MODEL (IWFM)
C                        *** Version 3.0 ***
C
C*******************************************************************************
C
C                          ZBUDGET INPUT FILE
C                        for IWFM Post-Processing
C
C
C             Project : IWFM, Version 3.0
C                       California Department of Water Resources
C                       February 2007
C             Filename: ZBUDMAIN.IN
C
C*******************************************************************************
C
C                            File Description
C
C    This file contains the name and description of the binary input file,
C    conversion factors, information on zone numbering and output control options
C    in order to generate detailed water budget tables for different zones of
C    aquifer system.
C
C*******************************************************************************
C                   Input and Output Control Data
C
C    BINFILE ; Binary input file name generated by Simulation
C    DSSFILE ; DSS file to store the Z-Budget output;
C                * Leave blank if the text output is desired
C    ZEXTENT ; Extent of the the zone numbering
C                1 = Zone numbering is defined for horizontal plane and will be
C                     used for all aquifer layers
C                0 = Different zone numbering is specified for each aquifer layer
C    FACTVLOU; Factor to convert the volumetric unit of values stored in the
C               binary input file to the desired unit of output
C    UNITVLOU; Output unit of volume (8 characters max)
C
C-------------------------------------------------------------------------------
C    VALUE                     DESCRIPTION
C-------------------------------------------------------------------------------
     ZB_RHO32D.Bin             / BINFILE
                               / DSSFILE
     1                         / ZEXTENT
     0.000022956               / FACTVLOU
     AC.FT.                    / UNITVLOU
C*******************************************************************************
C                    Output Cache Size
C
C    CACHE;   Cache size in terms of number of values stored for time series
C             data output
C
C-------------------------------------------------------------------------------
C   VALUE                        DESCRIPTION
C-------------------------------------------------------------------------------
    50000                        / CACHE
C*******************************************************************************
C                      Z-Budget Output Control Options
C                    (Simulation Date and Time NOT Tracked)
C
C    If the actual simulation date and time is NOT tracked enter the following
C    variables. Otherwise, comment out the following variables and use the
C    "Simulation Date and Time Tracked" option below.
C
C    TBEGIN ; Beginning time for the budget tables
C               * Use ##.# format
C    TLAST  ; Ending time for the budget tables
C               * Use ##.# format
C
C-------------------------------------------------------------------------------
C   VALUE                        DESCRIPTION
C-------------------------------------------------------------------------------
*                               / TBEGIN
*                               / TLAST
C-------------------------------------------------------------------------------
C                      Z-Budget Output Control Options
C                    (Simulation Date and Time Tracked)
C
C    If the actual simulation date and time is tracked enter the following
C    variables. Otherwise, comment out the following variables and use the
C    "Simulation Date and Time NOT Tracked" option above.
C
C    BDT    ; Begining date and time for the budget output
C               * Use MM/DD/YYYY_HH:MM format
C               * Midnight is 24:00
C    EDT    ; Ending date and time for the budget output
C               * Use MM/DD/YYYY_HH:MM format
C               * Midnight is 24:00
C
```

```
C-------------------------------------------------------------------------------
C   VALUE                       DESCRIPTION
C-------------------------------------------------------------------------------
   09/30/1921_24:00            / BDT
   09/30/1922_24:00            / EDT
C*******************************************************************************
C                     Zone Information
C
C    The following lists the zone numbers that the elements of the finite element
C    mesh belong to.  Element number, aquifer layer number (this information is
C    optional depending on the value of ZEXTENT above) and the zone number that
C    the element belongs to are required information. It is not necessary to list
C    all elements at all aquifer layers and assign a zone number to each of them.
C    By default, each element is given a zone number of -99.  Therefore, any elements
C    that are not listed below will constitute zone -99.
C
C    ** Note: If variable ZEXTENT above is set to 1, do not specify LAYER below. If
C             ZEXTENT is set to 0, it is required that LAYER for each element below
C             is specified.
C
C    IE   ; Element number
C    LAYER; Aquifer layer number at which element is located
C    ZONE ; Zone number
C
C-------------------------------------------------------------------------------
C    IE         LAYER        ZONE
C-------------------------------------------------------------------------------
     1378                    1
     1379                    1
     1386                    2
     1387                    2
     1390                    2
C*******************************************************************************
C                         Zone Print Options
C
C   The following lists the zone numbers for which a detailed water budget
C   print-out is desired.
C
C   ZPRINT; Zone number for budget print-out
C
C-------------------------------------------------------------------------------
C   ZPRINT
C-------------------------------------------------------------------------------
      1
      2
```

## 4.2. Output Files

Z-Budget creates two output files: the standard output file named ZBUDGETMESSAGES.OUT and the budget file that lists the detailed water budget information for the zones for which water budgeting is requested. Depending on the options specified in the main input file, the budget file can be an ASCII text file or a DSS file.

### Standard Output File (ZBudgetMessages.out)

This file lists information about the execution of Z-Budget. Errors or warning messages are printed in this file as well as the information for the successful completion of the program. Always check this file to make sure that the Z-Budget run was successful.

### Water Budget Output File

This file lists the detailed inflow and outflow terms to and from each of the zones for which a print-out is requested in the main control file. It can be an ASCII text or a DSS file depending on if an output DSS file name has been specified in the main control input file. If no DSS file name as for output file is specified, then an ASCII output text file is created. The name of this file is created by replacing the extension of the binary file name by the new extension ".BUD". For instance, if the name of the binary file is ZB.BIN, then the tabulated water budget values will be listed in the file ZB.BUD.

For each zone for which a print-out is obtained, the number of the inflow/outflow columns depends on the sources/sinks and types of boundary conditions included in the

simulation as well as the number of adjacent zones to the particular zone in hand. Some inflow/outflow components are common for all applications, whereas others are application specific. Table 4 is a list of all the inflow/outflow components that are addressed by IWFM and may appear in the zonal water budget tables. Due to the physical nature of these flow components, some of them can only be considered as an inflow to a zone, some of them are only outflow from a zone and some of them can be both inflow and outflow to or from a zone. This characteristic of each of the flow component is also listed in Table 4. A portion of a representative water budget output for a two subregion (subregions 1 and 2) system is shown below.

If a file name for DSS output file is specified in the main control input file, then the zonal flow terms are written to this DSS file using pathnames that are generated by Z-Budget. It should be noted that DSS file output option is available only if the Simulation was run using time-tracking option. The parts of the pathnames stored in the DSS output file are specified as follows:

**Part A:**

*IWFM_Z-BUDGET*

**Part B:**

*Zone: XXX* where *XXX* is the zone ID

**Part C:**

*VOLUME*

| Flow Component | Availability | Inflow or Outflow |
|---|---|---|
| Groundwater storage | All applications | Inflow/Outflow |
| Vertical flow among aquifer layers | Multi-layer systems | Inflow/Outflow |
| Seepage to/from streams | Available if the process is modeled | Inflow/Outflow |
| Tile drains | " | Outflow |
| Subsurface irrigation | " | Inflow |
| Subsidence | " | Inflow/Outflow |
| Net deep percolation | " | Inflow |
| Specified flow boundary condition | " | Inflow/Outflow |
| Specified head boundary condition | " | Inflow/Outflow |
| Rating table boundary condition | " | Inflow/Outflow |
| General head boundary condition | " | Inflow/Outflow |
| Baseflow from adjacent small watersheds | " | Inflow |
| Percolation from small watersheds | " | Inflow |
| Recoverable losses from diversions | " | Inflow |
| Recoverable losses from bypasses | " | Inflow |
| Seepage to/from lakes | " | Inflow/Outflow |
| Element pumping | " | Inflow/Outflow |
| Well pumping | " | Inflow/Outflow |
| Horizontal flows to/from adjacent zones | Available if more than 1 zone specified | Inflow/Outflow |

**Table 4.** Types of flow components available in Z-Budget output files

**Part D:**

Start date of the time series depending on the time step used in the Simulation and the value of the BDT variable (starting date and time for the printing of zonal flow terms) set in the Z-Budget main control input file

**Part E:**

Time step used in the Simulation

**Part F:**

Depending on the flow process, one of the items listed below:

i. *GW STORAGE_IN (_OUT)*

ii. *STREAMS_IN (_OUT)*

iii. *TILE DRAINS_IN (_OUT)*

iv. *SUBSURFACE IRRIGATION_IN (_OUT)*

v. *SUBSIDENCE_IN (_OUT)*

vi. *NET DEEP PERCOLATION_IN (_OUT)*

vii. *SPECIFIED FLOW BC_IN (_OUT)*

viii. *SPECIFIED HEAD BC_IN (_OUT)*

ix. *RATING TABLE BC_IN (_OUT)*

x. *GENERAL HEAD BC_IN (_OUT)*

xi. *SMALL WATERSHED BASEFLOW_IN (_OUT)*

xii. *SMALL WATERSHED PERCOLATION_IN (_OUT)*

xiii. *DIVERSION RECOVERABLE LOSS_IN (_OUT)*

xiv. *BYPASS RECOVERABLE LOSS_IN (_OUT)*

xv. *LAKES_IN (_OUT)*

xvi. *PUMPING BY ELEMENT_IN (_OUT)*

xvii. *PUMPING BY WELL_IN (_OUT)*

xviii. *VERTICAL FLOWS_IN (_OUT)*

xix. *FLOW FROM ZONE XXX_IN (_OUT)*

xx. *DISCREPANCY(IN-OUT)*

IWFM (v3.0)
ZONE BUDGET IN AC.FT. FOR ZONE 1

| Time | GW Storage | | ... | Pumping by Element | | Subsurface Flows: Zones 1 and -99 | | Subsurface Flows: Zones 1 and 2 | | Overall Zone Error |
|---|---|---|---|---|---|---|---|---|---|---|
| | IN | OUT | ... | IN | OUT | IN | OUT | IN | OUT | Sum(IN-OUT) |
| 10/31/1921_24:00 | 12373.0426 | 19629.6568 | ... | 0.0000 | 1388.6198 | 0.0000 | 30484.0599 | 19448.5529 | 0.0000 | 0.0000 |
| 11/30/1921_24:00 | 11931.8613 | 17557.3446 | ... | 0.0000 | 0.0000 | 0.0000 | 29935.3383 | 18929.9333 | 0.0000 | 0.0000 |
| 12/31/1921_24:00 | 11589.5588 | 15610.0159 | ... | 0.0000 | 0.0000 | 0.0000 | 29079.7310 | 18523.9647 | 0.0000 | 0.0000 |
| 01/31/1922_24:00 | 11185.0451 | 14029.5039 | ... | 0.0000 | 0.0000 | 0.0000 | 28245.4507 | 18123.1002 | 0.0000 | 0.0000 |
| 02/28/1922_24:00 | 10745.5500 | 12694.1383 | ... | 0.0000 | 0.0000 | 0.0000 | 27419.6176 | 17734.2649 | 0.0000 | 0.0000 |
| 03/31/1922_24:00 | 10281.9374 | 11523.6362 | ... | 0.0000 | 0.0000 | 0.0000 | 26661.3811 | 17357.3661 | 0.0000 | 0.0000 |
| 04/30/1922_24:00 | 9821.4266 | 10487.8552 | ... | 0.0000 | 0.0000 | 0.0000 | 25948.6139 | 16994.9576 | 0.0000 | 0.0000 |
| 05/31/1922_24:00 | 9363.8771 | 9579.1095 | ... | 0.0000 | 0.0000 | 0.0000 | 25263.9710 | 16646.2136 | 0.0000 | 0.0000 |
| 06/30/1922_24:00 | 8934.7275 | 8562.1944 | ... | 0.0000 | 287.5110 | 0.0000 | 24582.8178 | 16337.9089 | 0.0000 | 0.0000 |
| 07/31/1922_24:00 | 8489.0431 | 7893.4537 | ... | 0.0000 | 0.0000 | 0.0000 | 24172.9139 | 16005.8055 | 0.0000 | 0.0000 |
| 08/31/1922_24:00 | 8076.7292 | 7159.2041 | ... | 0.0000 | 7.6974 | 0.0000 | 23685.2067 | 15715.4895 | 0.0000 | 0.0000 |
| 09/30/1922_24:00 | 7681.7953 | 6655.8660 | ... | 0.0000 | 0.0000 | 29.3898 | 23080.0824 | 15415.8803 | 0.0000 | 0.0000 |

IWFM (v3.0)
ZONE BUDGET IN AC.FT. FOR ZONE 2

| Time | GW Storage | | ... | Pumping by Element | | Subsurface Flows: Zones 2 and -99 | | Subsurface Flows: Zones 2 and 1 | | Overall Zone Error |
|---|---|---|---|---|---|---|---|---|---|---|
| | IN | OUT | ... | IN | OUT | IN | OUT | IN | OUT | Sum(IN-OUT) |
| 10/31/1921_24:00 | 35205.0660 | 67171.0626 | ... | 0.0000 | 2082.9297 | 0.0000 | 30980.1457 | 0.0000 | 19448.5529 | 0.0000 |
| 11/30/1921_24:00 | 35675.2205 | 61185.6578 | ... | 0.0000 | 0.0000 | 0.0000 | 30484.5455 | 0.0000 | 18929.9333 | 0.0000 |
| 12/31/1921_24:00 | 35856.1736 | 54567.4622 | ... | 0.0000 | 0.0000 | 0.0000 | 30290.7689 | 0.0000 | 18523.9647 | 0.0000 |
| 01/31/1922_24:00 | 35747.6985 | 49308.8707 | ... | 0.0000 | 0.0000 | 0.0000 | 29664.9214 | 0.0000 | 18123.1002 | 0.0000 |
| 02/28/1922_24:00 | 35525.8867 | 45061.8649 | ... | 0.0000 | 0.0000 | 0.0000 | 28861.5755 | 0.0000 | 17734.2649 | 0.0000 |
| 03/31/1922_24:00 | 35413.9016 | 41744.4788 | ... | 0.0000 | 0.0000 | 0.0000 | 27997.2159 | 0.0000 | 17357.3661 | 0.0000 |
| 04/30/1922_24:00 | 35136.0593 | 38823.9824 | ... | 0.0000 | 0.0000 | 0.0000 | 27122.9893 | 0.0000 | 16994.9576 | 0.0000 |
| 05/31/1922_24:00 | 34733.0688 | 36295.4400 | ... | 0.0000 | 0.0000 | 0.0000 | 26199.8987 | 0.0000 | 16646.2136 | 0.0000 |
| 06/30/1922_24:00 | 34279.4051 | 33503.9719 | ... | 0.0000 | 431.2664 | 0.0000 | 25435.2009 | 0.0000 | 16337.9089 | 0.0000 |
| 07/31/1922_24:00 | 33693.4401 | 31039.3306 | ... | 0.0000 | 0.0000 | 0.0000 | 25414.8253 | 0.0000 | 16005.8055 | 0.0000 |
| 08/31/1922_24:00 | 32375.6806 | 28820.0267 | ... | 0.0000 | 11.5461 | 0.0000 | 24978.1940 | 0.0000 | 15715.4895 | 0.0000 |
| 09/30/1922_24:00 | 31603.1900 | 28143.5006 | ... | 0.0000 | 0.0000 | 0.0000 | 23189.1086 | 0.0000 | 15415.8803 | 0.0000 |

# 5. References


Allen, M. B., Herrera, I., and Pinder, G. F. (1988). *Numerical modeling in science and engineering*. John Wiley & Sons Inc.

Bear, J. (1988). *Dynamics of fluids in porous media*. Dover Publications, Inc., New York.

Berger, R. C., and Howington, S. E. (2002). "Discrete fluxes and mass balance in finite elements." *J. Hydraul. Eng.*, 128(1), 87-92.

Carey, G. F. (1982). "Derivative calculation from finite element solutions." *Comput. Methods Appl. Mech. Eng.*, 35, 1-14.

Carey, G. F. (2002). "Some further properties of the superconvergent flux projection." *Commun. Numer. Meth. Eng.*, 18, 241-250.

Carey, G. F., Chow, S. S., and Seager, M. K. (1985). "Approximate boundary-flux calculations." *Comput. Methods Appl. Mech. Eng.*, 50, 107-120.

Chavent, G., and Jaffré, J. (1986). Mathematical models and finite elements for reservoir simulation, North-Holland, New York.

Chou, S. H., He, S., and Lin, W. W. (2004). "Conservative flux recovery from Q1 conforming finite element method on quadrilateral grids." *Numer. Meth. Part. Diff. Eq.*, 20(1), 104-127.

Cordes, C., and Kinzelbach, W. (1992). "Continuous groundwater velocity fields and path lines in linear, bilinear and trilinear finite elements." *Water Resour. Res.*, 28(11), 2903-2911.

DWR (2007). *Integrated Water Flow Model (IWFM v3.0): Theoretical documentation*. Hydrology Development Unit, Modeling Support Branch, Bay-Delta Office, Sacramento.

DWR (2007). "IWFM: Integrated Water Flow Model." <http://baydeltaoffice.water.ca.gov/modeling/hydrology/IWFM/index.cfm> (February 2007).

Harbaugh, A. W. (1990). *A computer program for calculating subregional water budgets using results from the U. S. Geological Survey modular three-dimensional ground-water flow model*. U. S. Geological Survey Open-File Report 90-392.

Hughes, T. J. R., Engel, G., Mazzei, L., and Larson, M. G. (2000). "The continuous Galerkin method is locally conservative." *J. Comput. Phys.*, 163(2), 467-488.

Lynch, D. R. (1984). "Mass conservation in finite element groundwater models." *Adv. Water Resour.*, 7(2), 67-75.

McDonald, M. G., and Harbaugh, A. W. (1988). *A moduler three-dimensional finite-difference ground-water flow model*. U. S. Geological Survey Techniques of Water Resources Investigations, book 6, chap. A1.

Mosé, R., Siegel, P., Ackerer, P., and Chavent, G. (1994). "Application of the mixed hybrid finite element approximation in a groundwater flow model: luxury or necessity?" *Water Resour. Res.*, 30(11), 3001-3012.

Yeh, G. T. (1981). "On the computation of Darcian velocity and mass balance in the finite element modeling of groundwater flow." *Water Resour. Res.*, 17(5), 1529-1534.